Molecular Crystals and Liquid Crystals
Publication details, including instructions for authors and subscription information:
http://www.tandfonline.com/loi/gmcl16

Measurements of the Bend and Splay Elastic Constants of Octyl-Cyanobiphenyl

Stephen W. Morris [a] , P. Palffy-muhoray [a] & D. A. Balzarini [a]
[a] Department of Physics, The University of British Columbia, Vancouver, B. C., Canada, V6T 2A6

Version of record first published: 20 Apr 2011.

To cite this article: Stephen W. Morris , P. Palffy-muhoray & D. A. Balzarini (1986): Measurements of the Bend and Splay Elastic Constants of Octyl-Cyanobiphenyl, Molecular Crystals and Liquid Crystals, 139:3-4, 263-280

To link to this article: http://dx.doi.org/10.1080/00268948608080132

Mol. Cryst. Liq. Cryst., 1986, Vol. 139, pp. 263–280
0026-8941/86/1394–0263/$20.00/0

Printed in the United States of America

Measurements of the Bend and Splay Elastic Constants of Octyl-Cyanobiphenyl

STEPHEN W. MORRIS, P. PALFFY-MUHORAY, and D. A. BALZARINI

Department of Physics, The University of British Columbia, Vancouver B. C. Canada V6T 2A6

(*Received February 27, 1986*)

The bend (K_{33}) and splay (K_{11}) elastic constants of octylcyanobiphenyl have been measured as a function of temperature using the electric field induced Freedericksz transition. We have made simultaneous measurements of the dielectric constants and birefringence of 8CB using a cell with homogeneous alignment. Dielectric constants were measured using an AC bridge, while the birefringence was obtained using an interferometric technique. The sample temperature was controlled to better than ± 0.1 mK. Both the dielectric and optical data were analysed to yield the splay and bend elastic constants and the critical exponent associated with the divergence of K_{33} near the Nematic to Smectic A phase transition. The validity of the assumption of linear elastic response at temperatures close to the phase transition is discussed.

Keywords: liquid, crystal, elastic, exponent, dielectric, birefringence

INTRODUCTION

In this paper we report measurements of the splay (K_{11}) and bend (K_{33}) elastic constants of the liquid crystal 4,4′-n-octylcyanobiphenyl (8CB) throughout its nematic range with particular emphasis on temperatures near the second order Nematic to Smectic-A (N-S_A) transition.

The experimental method utilised the electric field induced Freedericksz transition in a sample with homogeneous alignment. At a given temperature, the capacitance and birefringence of a sample cell were measured simultaneously as a function of applied voltage. The

splay constant was determined from the critical voltage at the onset of the Freedericksz transition, while the bend constant was found by fitting the cell response to linear elastic theory.

Novel features of the experiment were unusually good temperature control (better than ± 0.1 mK) and the simultaneous measurement of optical and dielectric response. From the capacitance and dielectric data not only the elastic constants K_{11} and K_{33} but also both principal dielectric constants $\epsilon_{\parallel}$ and $\epsilon_{\perp}$, and the birefringence Δn of the bulk sample material could be determined at each temperature.

Precise temperature control allowed for the study of the divergence of the bend elastic constant due to smectic fluctuations near the N-S_A transition[1] and for the measurement of the critical exponent associated with this divergence.[2] In addition, fitting cell response data to theory provides information about the accuracy of linear elasticity theory in samples where the smectic fluctuations may be quenched by sample deformations.[1,3]

THEORY

The sample cell constituted a parallel plate capacitor with area A and thickness L. As described below, the surfaces were treated so as to produce strong anchoring of the director in the plane of the plates. For the undeformed cell, the capacitance is $C_0 = \epsilon_{\perp}\epsilon_0 A/L$. The optical phase difference for beams propagating in a direction normal to the plates and polarized parallel and perpendicular to the alignment direction is $d_0 = 2\pi L\ \Delta n/\lambda$, where $\Delta n = n_{\parallel} - n_{\perp}$ and $n_{\parallel}$ and $n_{\perp}$ are the refractive indices. The Freedericksz transition at the critical applied voltage $V_c = \pi\sqrt{K_{11}/\epsilon_0\Delta\epsilon}$, where $\Delta\epsilon = \epsilon_{\parallel} - \epsilon_{\perp}$, marks the onset of the electric field induced deformation.

At voltages V above the critical voltage V_c, the capacitance C and the optical phase difference d are given by the parametric equations:[4]

$$v = \frac{2}{\pi}\sqrt{1 + \gamma\eta}\int_0^{\pi/2}\left\{\frac{(1 + \kappa\eta\sin^2\phi)}{(1 + \gamma\eta\sin^2\phi)(1 - \eta\sin^2\phi)}\right\}^{1/2} d\phi \quad (1)$$

$$c = \frac{\displaystyle\int_0^{\pi/2}\left\{\frac{(1 + \gamma\eta\sin^2\phi)(1 + \kappa\eta\sin^2\phi)}{(1 - \eta\sin^2\phi)}\right\}^{1/2} d\phi}{\displaystyle\int_0^{\pi/2}\left\{\frac{(1 + \kappa\eta\sin^2\phi)}{(1 + \gamma\eta\sin^2\phi)(1 - \eta\sin^2\phi)}\right\}^{1/2} d\phi} - 1 \quad (2)$$

$$\delta = \frac{n_\parallel}{\Delta n}\left[1 - \frac{\int_0^{\pi/2}\left\{\frac{(1+\kappa\eta\sin^2\phi)(1+\gamma\eta\sin^2\phi)}{(1+\nu\eta\sin^2\phi)(1-\eta\sin^2\phi)}\right\}^{1/2} d\phi}{\int_0^{\pi/2}\left\{\frac{(1+\kappa\eta\sin^2\phi)(1+\gamma\eta\sin^2\phi)}{(1-\eta\sin^2\phi)}\right\}^{1/2} d\phi}\right] \tag{3}$$

in terms of the reduced quantities:

$$\gamma = \frac{\epsilon_\parallel}{\epsilon_\perp} - 1, \qquad \kappa = \frac{K_{33}}{K_{11}} - 1, \qquad \nu = \left(\frac{n_\parallel}{n_\perp}\right)^2 - 1$$

$$c = \frac{C}{C_0} - 1, \qquad \delta = 1 - \frac{d}{d_0}, \quad \text{and} \quad v = \frac{\dot{V}}{V_c} - 1.$$

The parameter η is given by $\eta = \sin^2\phi_m$, where ϕ_m is the angle between the director at the center of the cell and the direction perpendicular to the plates. In practice it is found that at large applied voltages the parameter η approaches unity, and numerical integration of the above integrals is difficult. A practical method for the evaluation of these integrals is described in the Appendix.

In the high voltage limit one finds[5] that the capacitance C varies linearly with $1/V$; that is,

$$C = C_\infty + S/V \tag{4}$$

where the intercept $C_\infty = \epsilon_\parallel \epsilon_0 A/L$. The slope S is an integral expression involving κ, γ, C_0 and V_c independent of A/L.

The birefringence case has a similar high voltage limit.[6] The birefringence of the deformed sample is obtained by measuring the intensity of light transmitted by the sample cell between crossed polarizers. The intensity of transmitted light is given by

$$I = I_0(1 - \cos(d)) \tag{5}$$

where d is the optical phase difference for the cell with the deformed sample.

EXPERIMENT

The cell was a transparent parallel-plate capacitor consisting of two circular In-SnO_2 (ITO) plates on glass blocks separated by a thin

mylar gasket. The plates were formed by etching ITO coated glass; the plate diameter was 0.50 in. The plate separation was measured by an interferometric technique[7] after the cell was filled and was found to be 39.5 μm with a variation in uniformity of less than ± 0.5 μm.

The inside surfaces of the capacitor were treated by oblique deposition from the vapour of a 400 Å thick SiO film at an angle of 30° from the normal to produce strong homogeneous alignment.[8]

The 8CB sample used to fill the cell was obtained from BDH and was used without further purification.

The glass blocks were clamped together by a copper cell body permitting electrical and optical access. The cell was housed in a solid copper cylinder 4 in. in diameter and 4 in. long with astatically wound heater coils on the outside. This cylinder was enclosed by styrofoam and was housed in a larger cylindrical copper can which formed the second stage of the temperature control.

The inner cylinder was temperature controlled to within ± .1 mK by a proportional-integral controller[9] which sensed the temperature with a Fenwall thermistor. The temperature was monitored with a second thermistor in a nulled bridge configuration which could detect temperature variations of 50 μK. The absolute temperature was obtained with a Hewlett-Packard 2804A quartz thermometer. It was calibrated to a Jarrett water triple-point cell and is believed to be absolutely accurate to within ±0.1 mK over the course of the experiment.

The outer can was temperature controlled to within ±1 mK by a large circulating water bath. Its controller used a thermistor placed on the can to determine the duty-cycle of a circuit which switched between a heater and a refrigerator. The can temperature was held 4K below that of the inner stage.

In the experiment, the temperature of the cell was held constant. The capacitance of the cell and the intensity of HeNe laser light transmitted by the cell between crossed polarizers was then measured as function of the amplitude of 1.5 kHz sinusoidal voltage applied to the cell. The amplitude of the applied voltage must change very slowly in time in order that the nematic orientation remain in equilibrium with the resulting electric field.

The experiment was controlled and the data was collected by a Commodore PET microcomputer via an IEEE bus system. Control of the amplitude of the applied voltage was carried out by the PET driving a 12-bit DAC whose output was filtered and used to amplitude modulate the output of an HP3312A signal generator. The internal

clock of the PET timed the step-rate of the DAC. The amplitude of the AC voltage across the cell could thus be ramped up or down at variable rates. The ramp rate required to keep the cell in near-equilibrium with the field was determined by requiring that no hysteresis be seen in the cell response. Near the Freedericksz transition, the ramp rate used was less than 0.05 mV/s.

The output of the signal generator was amplified and applied to the ratio transformer which forms the two arms of a General Radio 1615-A capacitance bridge. The transformer ratio was accurately unity. The voltage was measured by a Keithley 175 voltmeter under control of the PET. This was done on the primary side in order to avoid including the voltmeter capacitance in the bridge. The capacitance of the cell was measured by balancing the cell against standard capacitors in the bridge using a PAR 5204 vector lock-in amplifier in vector mode as null detector. The capacitance bridge was nulled manually and the capacitance was typed into the computer. The bridge was used in the shielded unknown configuration where the lead capacitances are excluded from the measurement; the cell capacitance was in the range of 200pF to 450pF and was measured to better than ± 0.01pF.

Data from optical measurements was collected by the PET simultaneously with the capacitance measurements. Attenuated light from a 0.5 mW Hughes HeNe laser polarized at 45° from the direction of alignment of the undistorted cell and propagating in a direction normal to the cell windows was passed through the cell and a crossed analyser. The intensity of the transmitted light was sensed by a phototransistor whose amplified output was measured by a Keithley 177 voltmeter on the IEEE bus and was recorded by the computer. The experiment could be visually monitored by observing the optical response of the cell on an x-y recorder.

DATA ANALYSIS

I. Capacitance measurements

Typical cell capacitance versus applied voltage data is shown in Figure 1a. The zero voltage capacitance C_0 was found by fitting the data at voltages below the Freedericksz transition to a straight line and taking the zero voltage intercept to be C_0. The capacitance above and near the transition (up to about $2V_c$ excluding the small region of rounding at V_c) was fitted to a quadratic function of the voltage; the intersection

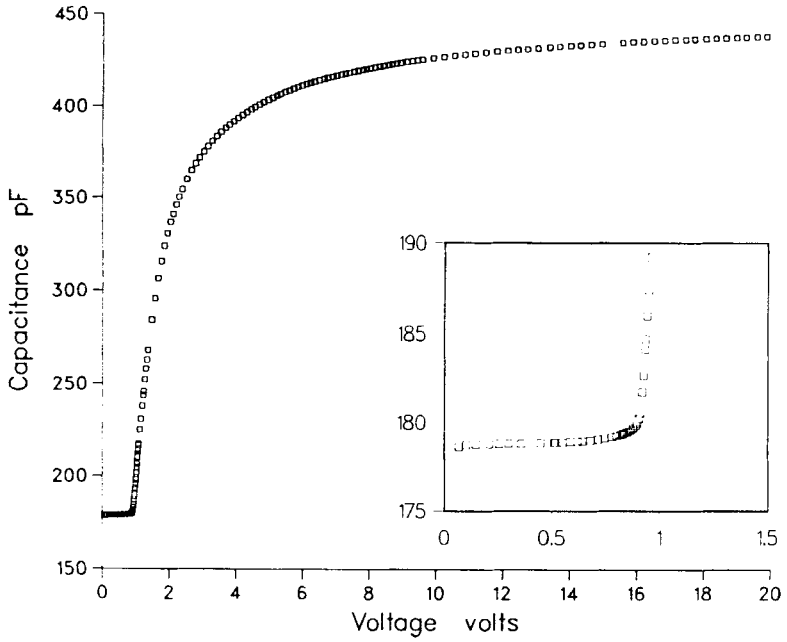

FIGURE 1a. Cell capacitance as function of applied voltage.

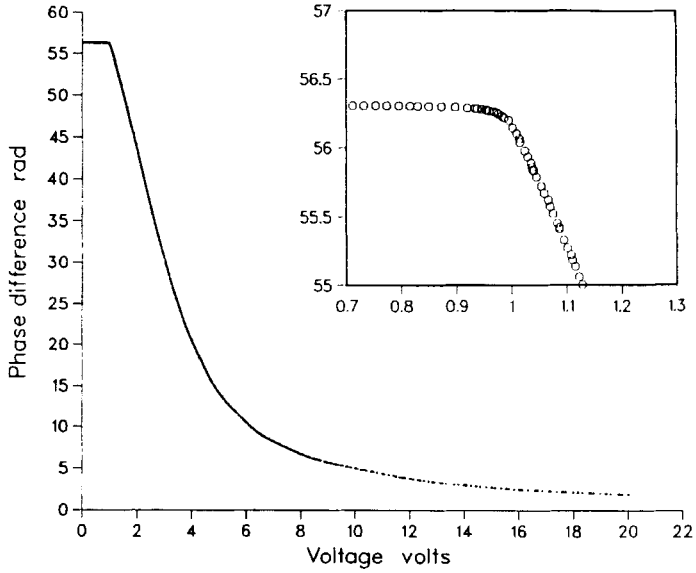

FIGURE 1b. Optical phase difference as function of applied voltage.

of this parabola with the straight line was used to determine the initial estimate of V_c. The coefficient of the linear term of the quadratic was used to determine the initial value of κ from the low voltage limit of Eqs. (1) and (2).[10] These initial estimates were used as starting values in an iterative non-linear least squares fit routine.

As expected from the high voltage limit of Eqs. (1) and (2), the capacitance is nearly linear with inverse voltage at high voltages. Typical data illustrating this is shown in Figure 2. A linear fit to data above a cutoff voltage (typically 17V) in this region was used to determine C_∞, the extrapolated capacitance at infinite voltage. This determines $\gamma = C_\infty/C_0 - 1$. The slope of the line gives an interesting high voltage measure of κ which is discussed below. C_0 and C_∞ give values of the dielectric constants given the area to thickness ratio of the cell. Since the uncertainty in our area to thickness ratio was relatively large, the value of this ratio was chosen within our uncertainty so that the values of $\epsilon_\perp$ agreed well with those of Dunmur[11] for 8CB. The dielectric constants are shown in Figure 3a. Figure 3b shows γ versus temperature. In principle, all the parameters necessary for the elastic constant calculation can be extracted from the capacitance data itself.

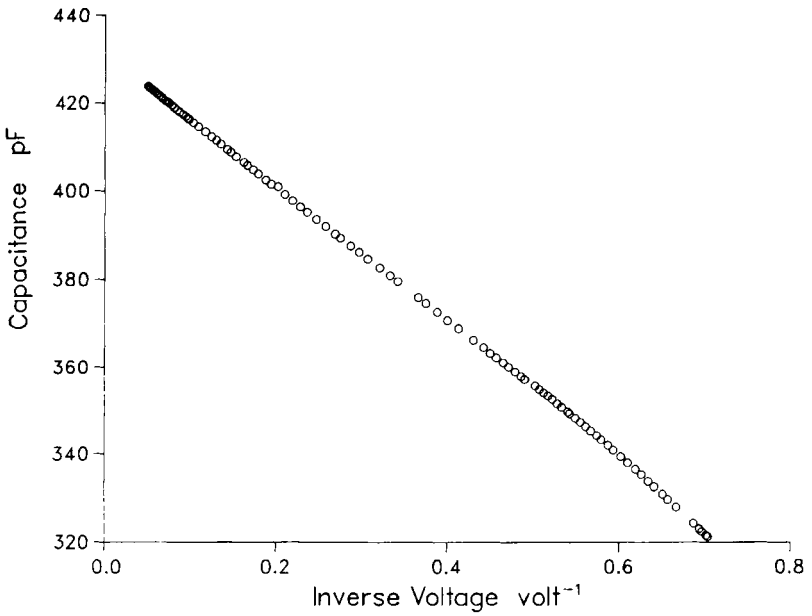

FIGURE 2. Cell capacitance as function of reciprocal of applied voltage.

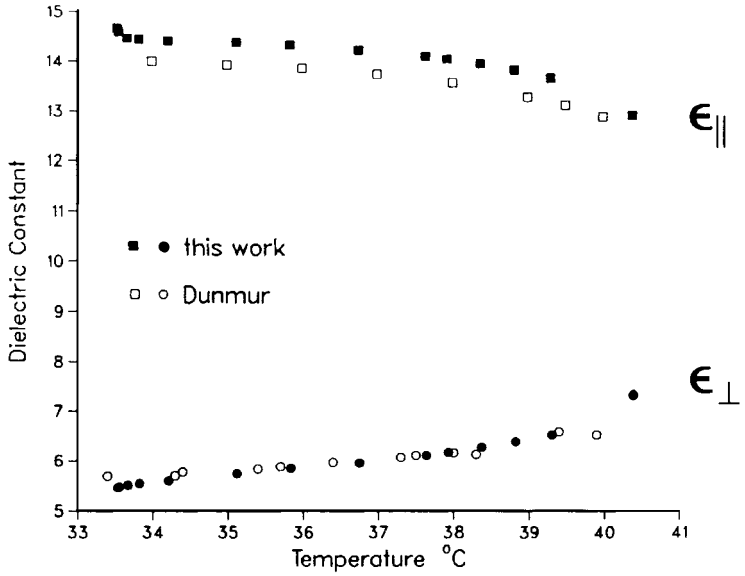

FIGURE 3a. Dielectric constants as functions of temperature.

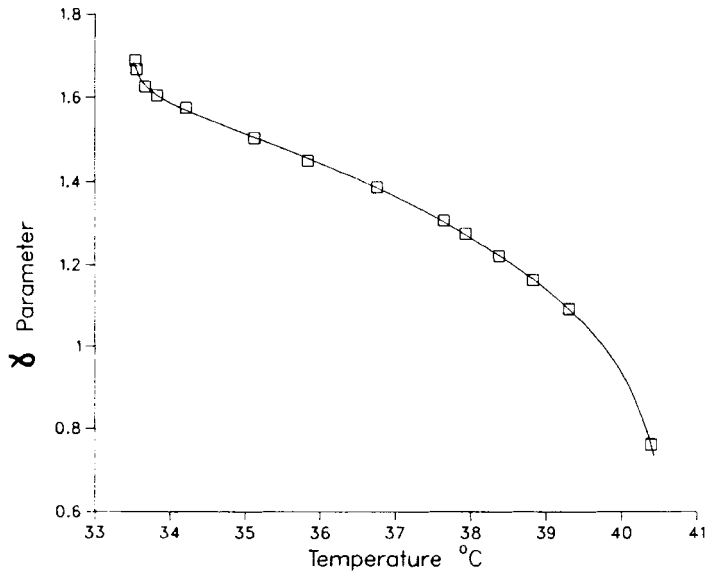

FIGURE 3b. Reduced dielectric constant γ as a function of temperature.

II. Optical measurements

In the optical data analysis, the phase difference d was first obtained from the transmitted intensity measurements from Eq. (5). Since I_0 in Eq. (5) was found to vary with voltage, a piecewise linear envelope was fitted to the extrema of the oscillating intensity versus voltage curves. Under the assumption that I_0 is only weakly varying function of V, Eq. (5) may be inverted to determine $d(V)$; typical results are shown in Figure (1b). At temperatures very near ($\simeq$ 50 mK) the N-I and the N-S_A transitions, scattering and depolarization cause this assumption to break down, and the uncertainties in $d(V)$ become large. Data at voltages below V_c gives information about the zero voltage phase difference d_0 and hence Δn if the cell thickness to wavelength ratio L/λ is known. The initial values of d_0, V_c and κ were determined from the raw phase data by a method similar to the capacitance case.

The temperature dependence of Δn is shown in Figure (4b). We have used Dunmur's values[11] of the average index $\bar{n} = (n_\parallel + 2n_\perp)/3$ and our Δn to determine $n_\parallel$ and $n_\perp$, and hence the reduced index v. These are shown in Figure (4a).

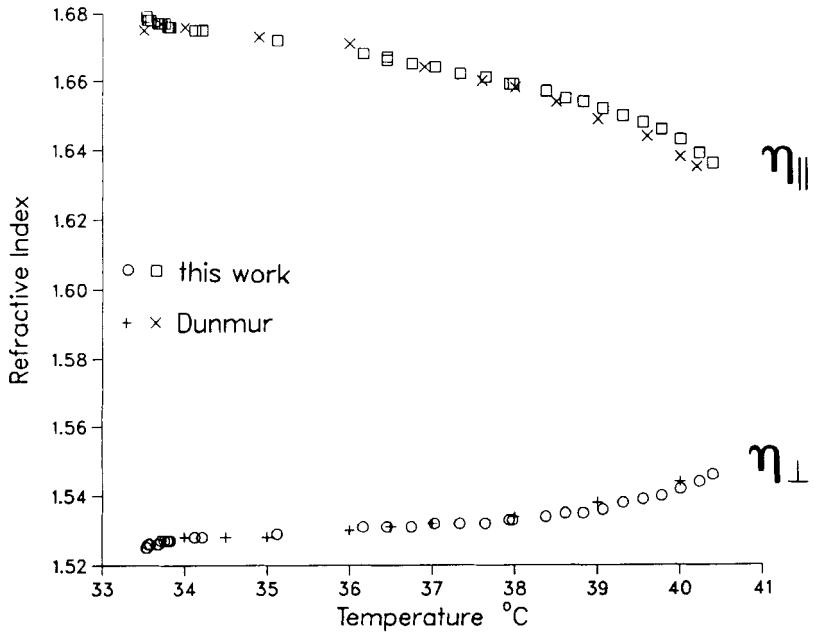

FIGURE 4a. Refractive indices as functions of temperature.

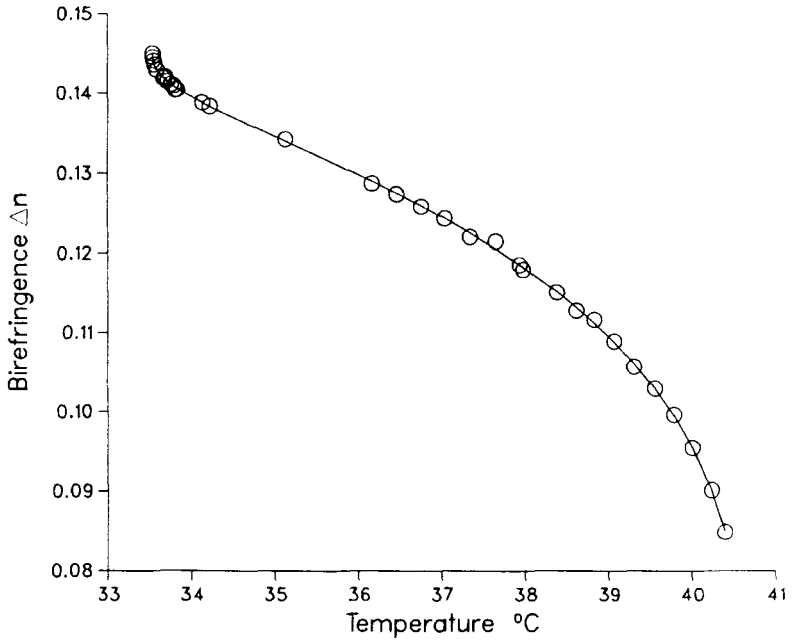

FIGURE 4b. Birefringence Δn as a function of temperature.

III. Curve fitting

The non-linear fitting procedure was similar for capacitance and optical data. It has been found[12,13] that multi-parameter fitting to the Deuling theory is poorly conditioned and it is therefore desirable to fix as many parameters as possible. Our non-linear fit program varies κ and V_c while keeping γ, ν, C_0 and d_0 fixed. The search routine used was a simple parabolic extrapolation scheme[14] which was arranged to have as few calls as possible to the goodness-of-fit function to be minimized.

We took this function to be the sum of the squares of the least distance (the 'perpendicular' residuals) between each data point and the theoretical curve. This approach was motivated by the desire to ensure that the data was not systematically weighted by the fitting procedure as is the case with the more commonly used 'vertical' residuals,[15] which are the distances between each data point and the theoretical curve in a direction parallel to one of the coordinate axes. The use of residuals measured along the capacitance or phase difference axes would strongly weigh the data in favour of the points in the region of the initial steep rise in response over points elsewhere.

Typical fits and their perpendicular residuals are shown in Figures 5a and 5b. All the data up to $20V_c$ was fitted to theory. It is evident from Figures 5a and 5b that although the residuals are small, there are systematic deviations from a random distribution of residuals about the mean indicating that the theory does not completely describe the cell response. These trends are qualitatively similar to those observed by Maze.[13] The non-random distribution of residuals is usually dealt with by 'range-shrinking,' where data is fit only below a cutoff voltage ($2V_c$) chosen so that the residuals in this range are indeed random.[13]

In our present analysis, we have not carried out range-shrinking. We find that our values of $\epsilon_{\parallel}$ found from the extrapolation to infinite

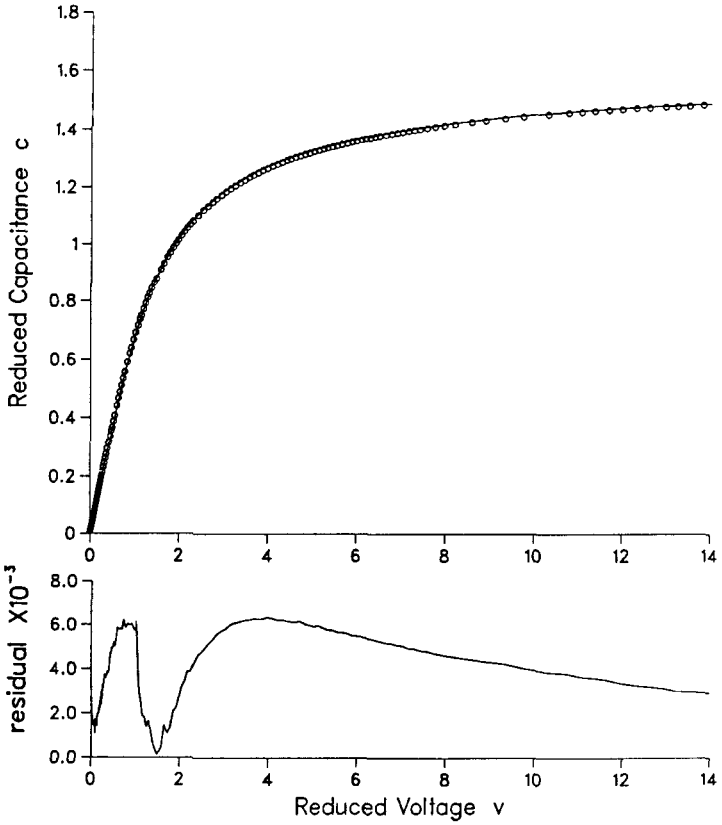

FIGURE 5a. Fit from theory (solid line) to reduced capacitance data (circles). The residuals are shown below.

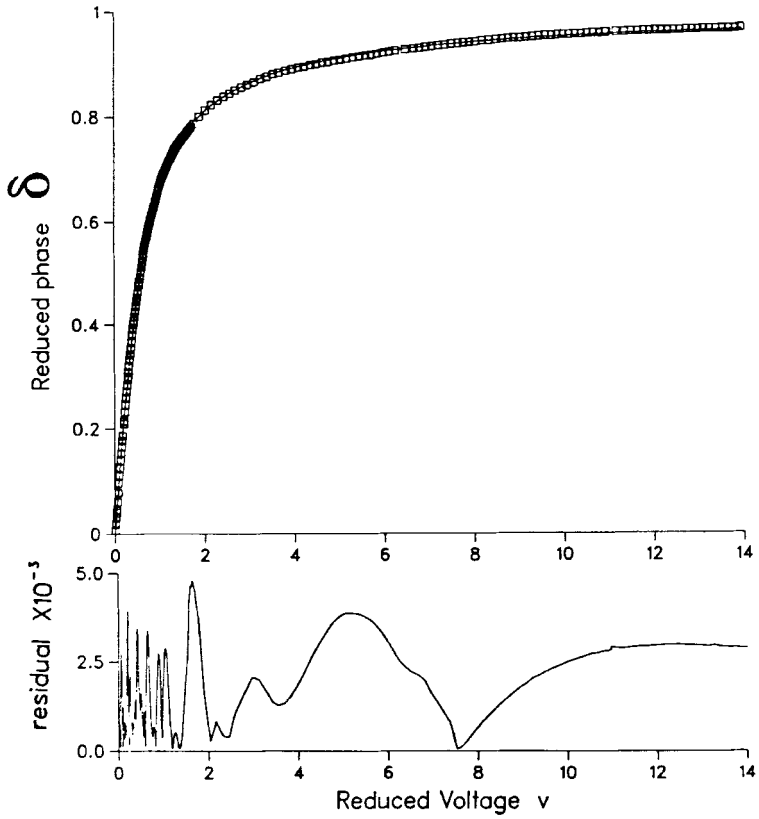

FIGURE 5b. Fit from theory (solid line) to reduced optical phase data (squares). The residuals are shown below.

voltage are systematically larger than those of Dunmur[11] which were obtained with a homeotropically aligned cell at low voltages. We also found that the values of κ obtained from the high voltage analysis[5] were systematically larger than those from the full non-linear fits. These results suggest that the cell response at high voltages might be viewed as being well described by the Deuling theory,[4] but with values of γ and κ which are larger than the zero-field values. The trends seen in the residuals could then be attributed to a weak dependence of the dielectric and elastic constants of the sample material on the electric field and on sample deformation. We have also found that the goodness of fit is strongly temperature dependent. At temperatures near the N-S_A transition, the average size of the residuals increases significantly, and the region where the residuals are random

becomes smaller. Any cutoff voltage defining the region where the residuals are random would therefore have to depend on temperature.

In this paper we present the results of fitting the data over the entire range of voltages. The resulting elastic constants are shown in Figures (6) and (7). K_{33} shows the expected strong pretransitional divergence. K_{11} as well as γ and Δn show small pretransitional increases due to the effect of the smectic fluctuations on the nematic order parameter as can be seen on Figures 6, 3b and 4b.

From theory,[2] the temperature dependence of the bend elastic constant is given by

$$K_{33} = K_{33}^0 + At^{-x} \tag{6}$$

where $t = (T/T_{NA}) - 1$ is the reduced temperature, K_{33}^0 is the background nematic contribution, A is a 'bare' elastic constant and x is the critical exponent. This critical exponent is expected to be the same as the parallel correlation length exponent.[1]

Since T_{NA} was not directly measured in the experiment, it was determined from fitting the K_{33} values to Eq. (6). K_{33}^0 was chosen to

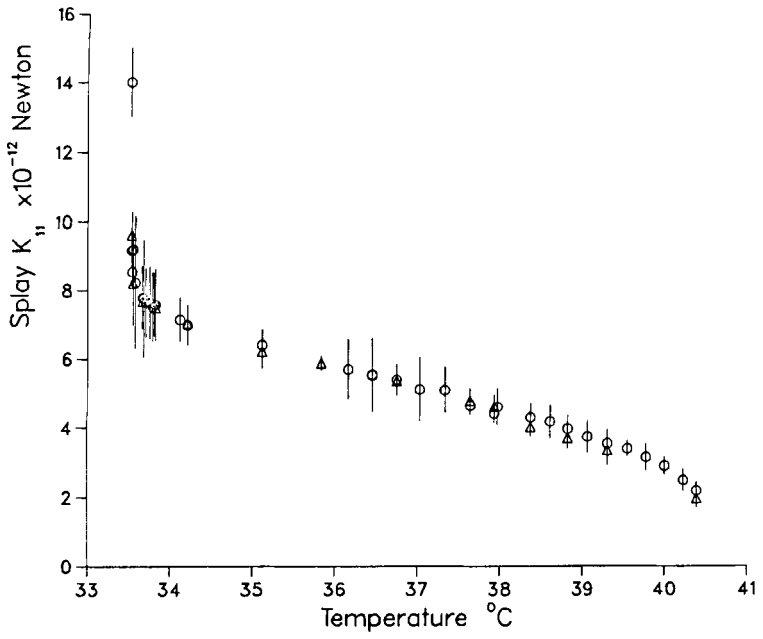

FIGURE 6. Splay elastic constant K_{11} as function of temperature from both optical phase (circles) and capacitance (triangles) results.

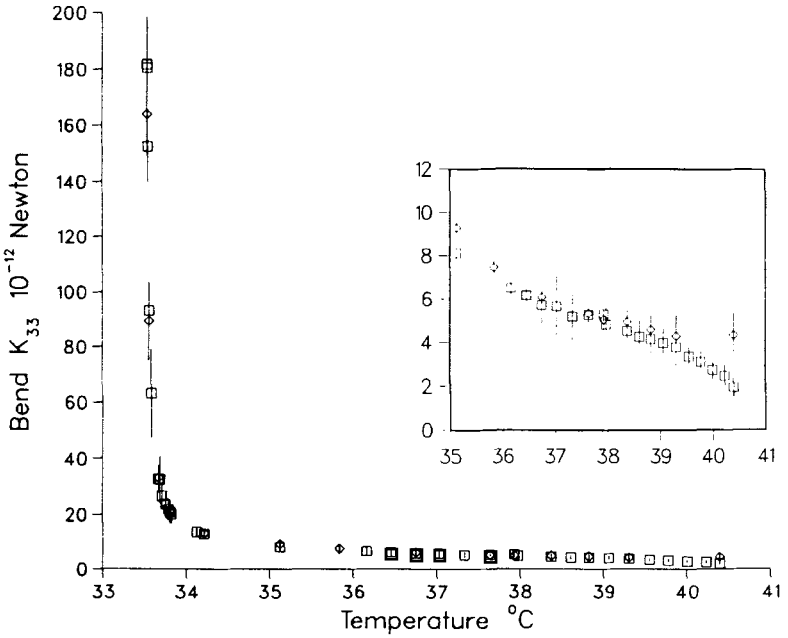

FIGURE 7. Bend elastic constant K_{33} as function of temperature from both optical phase (squares) and capacitance (diamonds) results.

be that part of $K_{33}(T)$ which is linear in Δn^2, since Δn^2 gives the classical nematic temperature dependence of K_{33}. The critical exponent x, however, is not sensitively dependent on K_{33}^0.[16] Figure 8 shows the best fit to the data, with $x = 1.0 \pm .1$ and $T_{NA} = 33.507 \pm .005$°C.

CONCLUSIONS

We have determined the bend and splay elastic constants of 8CB from simultaneous optical and dielectric measurements on a sample undergoing the electric field induced Freedericksz transition. The splay constant was determined from the critical voltage at which the transition occurs, while the bend constant was determined from the subsequent cell response up to voltages about twenty times the critical voltage.

As well as providing values of the elastic constants, dielectric constants and the birefringence as functions of temperature, the exper-

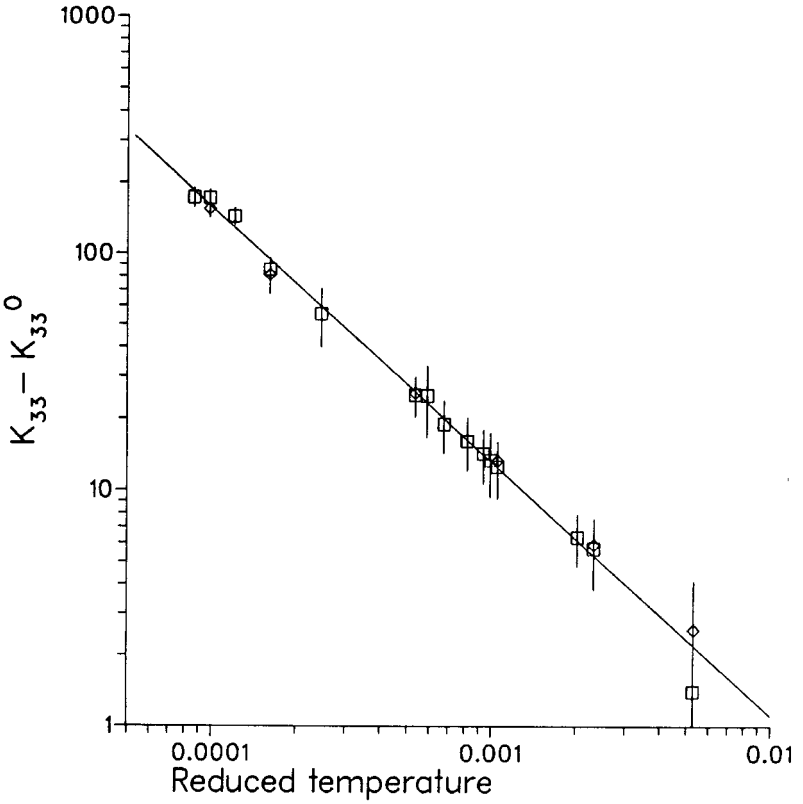

FIGURE 8. Best linear fit (solid line) to logarithm of the divergent part of the bend elastic constant K_{33} (diamonds denote capacitance results, squares denote optical phase results).

imental results constitute a test of theories of these physical properties. A region of particular interest is near the smectic *A* phase, where the bend elasticity is dominated by smectic fluctuation effects.

It was found that the elastic constants calculated from the optical and capacitance measurements agreed to within the associated uncertainty. The results from the optical measurements were found to be more accurate. In analyzing data over the entire range of voltages studied, we found systematic deviation from the Deuling theory[4] at all temperatures, similar to the observations of Maze.[13] Elastic constant values determined from the high voltage capacitance data were systematically larger than those obtained from fits at lower voltages. Extrapolation of the capacitance data to infinite voltage yielded values which were systematically larger than those measured by Dunmur[11]

at low fields. As the N-S_A transition was approached, the mean value of the residuals associated with fitting our data to theory increased, while the voltage range where the residuals were randomly distributed about the mean became narrower.

Some deviation of the experimentally observed cell response from theory may be explained if, as suggested by our results, the dielectric and elastic constants vary with the applied electric field. In the absence of deformations of the director field, the dependence of these constants on the electric field is expected to be small, except near the N-I transition. In our experiment, however, large electric fields are accompanied by curvature strains, and the combined effect of these on dielectric and elastic properties is less well understood.

These deviations also suggest the possibility of the breakdown of linear elasticity at large deformations and at temperatures close to the N-S_A transition. This breakdown could be due to the suppression of smectic fluctuations which are responsible for the divergence of K_{33} by deformations where the director field is not curl free.[1] This mechanism is responsible for the lowering of the N-S_A transition temperature by large curvature strains.[17] A mean-field theory of nonlinear elasticity has been proposed by Chu and McMillan;[18] we have not yet attempted to interpret our data within the framework of this theory.

The validity of the assumption of linear elastic response has been tested close to T_{NA} by Majoros et al.[3] using magnetic field induced formations. They found no disagreement with the linear theory above temperatures very close to T_{NA} where they observed the onset of a 'stripe instability'.[3,19] It is hypothesized that the instability signals the onset of nonlinear elastic behavior. In our experiment, the deformations were larger than those usually produced by magnetic fields. Direct comparison with magnetic deformation experiments are made difficult by systematic deviations of experimental results from predictions of the linear theory at high electric fields even far from T_{NA}. We did not observe any instabilities above the lowest reduced temperature of 8×10^{-5} which was reached. Nonetheless, we did observe significantly increased deviations from the linear theory as T_{NA} was approached.

The critical exponent for the divergence of K_{33} was found to be 1.0 ± 0.1. This value is in agreement with some early measurements using Freedericksz transitions,[20,21] but it is larger than light scattering[22,23] and X-ray[24,25] results which give values near 0.7. It is also in disagreement with the de Gennes prediction of 0.67. The discrepancy between our exponent and those obtained from measurements on

undistorted samples suggests that a more thorough understanding of dielectric and elastic properties of nematics in the presence of external fields and director field deformations is required.

Acknowledgments

We would like to thank J. R. de Bruyn, A. J. Berlinsky, B. Bergersen and D. Zimmerman for many useful discussions. The liquid crystal samples were provided by Dr. D. A. Dunmur. Some of the data collection was done by Alec Sandy and Don Mathewson. The bath temperature controller was designed and built by Kent Lundgren.

APPENDIX

Efficient evaluation of integrals

All three integrals are of the form:

$$I = \int_0^{\pi/2} \frac{f(\phi)d\phi}{\{1 - \eta\sin^2\phi\}^{1/2}}$$

for various well-behaved functions f. For voltages much greater than V_c, the parameter η becomes very nearly equal to 1. Since $f(\pi/2)$ is non zero, the largest contribution to the integral comes from values of ϕ very nearly equal to $\pi/2$. The complete elliptic integral of the first kind is:

$$K(\eta) = \int_0^{\pi/2} \frac{d\phi}{\{1 - \eta\sin^2\phi\}^{1/2}}$$

For η close to 1, $K(\eta)$ is given approximately by[26]

$$K(\eta) \simeq a_0 - b_0 \log(1 - \eta).$$

This suggests a new, natural parameter α where

$$\eta = 1 - e^{-\alpha}.$$

For high voltages, α varies more linearly with voltage than η. We rewrite the integral as:

$$I = e^{\alpha/2} \int_0^{\pi/2} \frac{\{f(\phi) - f(\pi/2)\}}{\{1 + (e^{\alpha} - 1)\cos^2\phi\}^{1/2}} d\phi + f(\pi/2)K(1 - e^{-\alpha}).$$

The integral in the above expression is well behaved and can be evaluated with standard integration routines, even for large α. The elliptic integral K depends only on α; its values are well tabulated or can be evaluated with a polynomial approximation.[26]

References

1. P. G. de Gennes, *Solid St. Comm.*, **10**, 753 (1972).
2. T. C. Lubensky, *J. de Chim. Phys.*, **80**, 31 (1983).
3. S. J. Majoros, D. J. Brisbin, D. L. Johnson and M. E. Neubert, *Phys. Rev. A.*, **20**, 1619 (1979).
4. H. J. Deuling, *Mol. Cryst. Liq. Cryst.*, **19**, 123 (1972).
5. T. Uchida, Y. Takahashi, *Mol. Cryst. Liq. Cryst. Lett.*, **72**, 133 (1981).
6. D. A. Balzarini, D. A. Dunmur and P. Palffy-Muhoray, *Mol. Cryst. Liq. Cryst. Lett.*, **102**, 35 (1984).
7. S. A. Casalnuovo, R. C. Mockler and W. J. O'Sullivan, *Phys. Rev. A.*, **29**, 257 (1984).
8. J. Cognard, 'Alignment of Nematic Liquid Crystals and their Mixtures,' (*Mol. Cryst. Liq. Cryst.* sup. 1), Gordon and Breach, New York (1982).
9. E. M. Forgan, *Cryogenics*, **14**, 207 (1974).
10. R. J. A. Trough and E. P. Raynes, *Mol. Cryst. Liq. Cryst. Lett.*, **56**, 19 (1979).
11. D. A. Dunmur, R. A. Manterfield, W. H. Miller and J. K. Dunleavy, *Mol. Cryst. Liq. Cryst.*, **46**, 127 (1978).
12. C. Maze and D. Johnson, *Mol. Cryst. Liq. Cryst.*, **33**, 213 (1976).
13. C. Maze, *Mol. Cryst. Liq. Cryst.*, **48**, 273 (1978).
14. P. R. Bevington, 'Data Reduction and Error Analysis for the Physical Sciences,' McGraw-Hill, New York (1969).
15. J. O'Rear, *Am. J. Phys.*, **50**, 912 (1982).
16. R. G. Priest, *Mol. Cryst. Liq. Cryst.*, **17**, 129 (1972).
17. N. V. Madhusudana and B. S. Srikanta, *Mol. Cryst. Liq. Cryst.*, **99**, 375 (1973).
18. K. C. Chu and W. L. McMillan, *Phys. Rev. A.*, **15**, 337 (1977).
19. P. E. Cladis and S. Torza, *J. Appl. Phys.*, **46**, 584 (1975).
20. I. Janossy and L. Bata, *Act. Phys. Pol.*, **A54**, 643 (1978).
21. L. Cheung and R. B. Meyer, *Phys. Lett.*, **43A**, 261 (1973).
22. S. Sprunt, L. Solomon and J. D. Litster, *Phys. Rev. Lett.*, **53**, 1923 (1984).
23. H. Bireki and J. D. Litster, *Mol. Cryst. Liq. Cryst.*, **42**, 1043 (1977).
24. B. M. Ocko, R. J. Birgenau and J. D. Litster, *Phys. Rev. Lett.*, **52**, 208 (1984).
25. C. W. Garland, M. Meichle, B. M. Ocko, A. R. Kortan, C. R. Safinya, L. J. Yu, J. D. Litster and R. J. Birgenau, *Phys. Rev. A.*, **27**, 3234 (1983).
26. M. Abramowitz and I. Stegun, 'Handbook of Mathematical Functions,' Dover, New York (1970).